Isothermal absorption of soluble gases by atmospheric nanoaerosols

T. Elperin,[*] A. Fominykh,[†] and B. Krasovitov[‡]
Department of Mechanical Engineering, The Pearlstone Center for Aeronautical Engineering Studies, Ben-Gurion University of the Negev, P.O. Box 653, 84105, Israel

A. Lushnikov[§]
Karpov Institute of Physical Chemistry, 10, Vorontsovo Pole, 105064 Moscow, Russia
(Received 13 September 2012; published 15 January 2013)

We investigate mass transfer during the isothermal absorption of atmospheric trace soluble gases by a single droplet whose size is comparable to the molecular mean free path in air at normal conditions. It is assumed that the trace reactant diffuses to the droplet surface and then reacts with the substances inside the droplet according to the first-order rate law. Our analysis applies a flux-matching theory of transport processes in gases and assumes constant thermophysical properties of the gases and liquids. We derive an integral equation of Volterra type for the transient molecular flux density to a liquid droplet and solve it numerically. Numerical calculations are performed for absorption of sulfur dioxide (SO_2), dinitrogen trioxide (N_2O_3), and chlorine (Cl_2) by liquid nanoaerosols accompanied by chemical dissociation reaction. It is shown that during gas absorption by nanoaerosols, the kinetic effects play a significant role, and neglecting kinetic effects leads to a significant overestimation of the soluble gas flux into a droplet during the entire period of gas absorption.

DOI: 10.1103/PhysRevE.87.012807 PACS number(s): 82.33.Tb, 92.60.Mt, 92.60.Nv

I. INTRODUCTION

Atmospheric aerosols are directly emitted into the atmosphere from natural or anthropogenic sources, or they can be formed in the atmosphere through the nucleation of gas-phase species. Aerosol nucleation events produce a large fraction of atmospheric aerosols. New particle formation occurs in two distinct stages, i.e., nucleation to form a critical nucleus and subsequent growth of the critical nucleus to a larger size (>2–3 nm) that competes with the capture and removal of the freshly nucleated nanoparticles by coagulation with pre-existing aerosols [1]. In the continental boundary layer, there are frequent observations of the formation of ultrafine aerosol particles accompanied by subsequent growth [2]. Gas absorption of soluble trace atmospheric gases by liquid atmospheric aerosol particles including ultrafine particles plays an important role in climate and atmospheric chemistry.

The consequence of aerosol climate forcing is that cooling can be intensified with increasing atmospheric amounts of water-soluble trace gases such as HNO_3, counteracting the warming effect of greenhouse gases [3]. Scavenging of atmospheric gaseous pollutants by cloud droplets is a result of the gas absorption mechanism [4,5]. Gas scavenging of highly soluble gases by atmospheric water droplets includes absorption of HNO_3,H_2O_2,H_2SO_4,HCL, and some other gases. The sources of these gases in the atmosphere are briefly reviewed in Refs. [6,7]. Soluble gas absorption by noncirculating droplets was investigated experimentally in Ref. [8], where conditions of noncirculation for falling liquid droplets were determined by employing water droplets with the Sauter mean diameter equal to 0.185, 0.148, and 0.137 mm.

Gas absorption by stagnant liquid droplets in the presence of inert admixtures when both phases affect mass transfer was analyzed in Ref. [9], pp. 54 and 55. The criterion of applicability of the steady-state assumption to the problem of simultaneous diffusion and aqueous-phase reaction was considered by Schwartz and Freiberg [10]. They showed that a condition for using a steady-state approximation for mass transport during gas absorption by a droplet reads

$$t \gg \tau_{\mathrm{reag}} = \frac{n_{L,\mathrm{eq}}}{R_{\max}}, \tag{1}$$

where t is the overall time of the process, τ_{reag} is the characteristic time of the reagent supply, $n_{L,\mathrm{eq}}$ is the equilibrium value of aqueous-phase reagent concentration, $R_{\max} = 3D_G n_{G,\mathrm{eq}}/a^2$ is the gaseous-phase diffusion-limited maximum rate, D_G is the gas-phase diffusion coefficient, $n_{G,\mathrm{eq}}$ is the equilibrium value of gas-phase bulk concentration, and a is the droplet radius. Equilibrium is attained when $t \gg \tau_{\mathrm{reag}}$ [10]. Scavenging of soluble gases by single evaporating droplets was studied in Refs. [11,12].

All the aforementioned works considered trace gas absorption in the continuous limit, where Fick's law relates the flux and the concentration gradient of reactant. Recently, some studies have attempted to describe the reactant transport in the gaseous phase in the free-molecular and transition regimes, where the droplet size is less than or comparable to the mean free path of the molecules in the gaseous phase. Discussion of recent results and approaches can be found in Refs. [6,13–16]. The existing attempts to describe the transitional and free-molecule regimes have encountered some difficulties in formulating the boundary conditions to the transport equations. For example, in Ref. [17] the diffusion equations and a microscopic boundary condition for describing the reactant transport toward the particle surface were used. The rigorous approach requires a solution of the full transport

[*]elperin@bgu.ac.il
[†]fominykh@bgu.ac.il
[‡]borisk@bgu.ac.il
[§]alex.lushnikov@mail.ru

problem, including the reactant transport in the gaseous phase and the gas-liquid interface, by solving the Boltzmann kinetic equation and the diffusion-reaction equation inside the droplet.

In this study, we employ a different approach for describing gas uptake by nanodroplets. We modify the flux-matching approach of Ref. [18] by including the in-particle chemical transformations of the reactant molecules. The results are applied for consideration of the trace gases scavenging by atmospheric aerosols.

Let us assume that the reactant molecules (A molecules) move toward the droplet which captures them. The ultimate fate of the reactant molecules depends on the results of the chemical reactions inside the particle. Let us denote by $n_\pm$ the concentrations of A molecules right outside (n_+) or right inside (n_-) the particle surface. Clearly, these concentrations $n_\pm$ depend on the nature of the physicochemical processes at the surface and inside the particle. Let n_∞ be the number density of A molecules far from the particle. It is commonly accepted that the concentration difference $n_\infty - n_+$ drives a flux of A molecules toward the particle surface. The mass of the particle begins to increase, and its chemical composition changes. The rate of change of the number of A molecules inside the particle is equal to the total flux J, i.e., the total number of molecules deposited per unit time at the particle surface minus the rate of consumption of molecules A by the chemical reaction inside the particle. Some fraction of A molecules is assumed to escape from the particles. In steady-state conditions, the flux J can be written as

$$J = \alpha(a)(n_\infty - n_+), \tag{2}$$

where $\alpha(a)$ is the capture efficiency and a is the particle radius. Clearly, the capture efficiency α depends on the mass accommodation coefficient S_p. The latter is defined as the probability for an A molecule to stick to the particle after a single collision. Since the interface and in-particle processes determine the value of n_+, Eq. (2) can be rewritten as follows [16]:

$$J = \frac{\alpha(a) n_\infty}{1 + \alpha(a)\psi(a,J)}, \tag{3}$$

where $\psi(a,J)$ is a function depending on the nature of the chemical reaction. In the case of the first-order chemical reaction, the function ψ is independent of J. However, if the chemical reaction inside the particle is of higher order, then J is a solution of the nonlinear algebraic equation (3). Note that we did not specify the functions $\alpha(a)$ and $\psi(a,J)$ in Eq. (3). The information on the processes at the surface and inside the particle is carried by the function $\psi(a,J)$. Hence, Eq. (3) is quite general. All further approximations concern the values of the uptake efficiency $\alpha(a)$ and the reaction function $\psi(a)$.

II. DESCRIPTION OF THE MODEL

A. Preliminary remarks

The characteristic times of changes of the number density of reactant A in gaseous and liquid phases differ by several orders of magnitude. In particular, the relaxation time inside the micrometer-sized droplet is $\tau_L \propto a^2/D_L \simeq 10^{-3}$ s, where $D_L \simeq 10^{-5}$ cm^2/s denotes the diffusivity of the reactant molecules in the liquid phase. The relaxation time in the gaseous phase can be estimated as $\tau_G \propto a/v_T \simeq 10^{-8}$ s, where v_T is the mean thermal velocity of the reactant molecules, $v_T \simeq 10^2$ m/s. Here one can use the free molecular estimate because the droplet size is of the order of the mean free path of the reactant molecule. Following [6], the characteristic time of diffusion in a gaseous phase, corresponding to the time required by gas-phase diffusion to establish a steady-state profile around a particle, can be alternatively estimated as $\tau_G \propto a^2/D_G \simeq 10^{-8}$ s. As can be seen from these estimates, the characteristic time of diffusion in a gaseous phase, τ_G, is much smaller than the characteristic time of diffusion in the liquid phase, τ_L, which is required for a saturation of the droplet by soluble gas (i.e., $\tau_G \ll \tau_L$). Therefore, for the large values of t ($t \gg \tau_G$), it is reasonable to assume that the concentration profile in a gaseous phase in the transitional regime and the flux attain their quasi-steady-state values [19] and are determined by Eq. (2) [or in more general form by Eq. (3)]. Schwartz and Freiberg [10] showed that regarding the mass transfer in a liquid phase for $t = \lambda^{-1}$ (where t is the overall time of the process and λ is the reaction rate), the mass flux differs from the steady-state value by ≈7%, and for $t = 2\lambda^{-1}$ the difference is 1.1% only. In the case of SO_2 absorption by a water droplet the magnitude of λ^{-1} is of the order of 10^3 s. These estimations show that in the case of nanoaerosols, the steady-state regime of mass transfer in an aqueous phase is not realized.

The molecular mean free path in air at normal conditions is $\ell \approx 65$ nm, i.e., it is comparable to the sizes of the nanometer droplets. This implies that the motion of the reactant molecules cannot be described as Fickian diffusion, and one must apply the Boltzmann kinetic theory. However, solving the Boltzmann equation analytically or numerically is a formidable task.

The idea of applying the flux-matching approach in aerosol kinetics was pioneered in Ref. [20] by Fuchs. His reasoning was quite simple. At a large distance from the droplet, the reactant transport can be described by the diffusion equation. In the vicinity of the droplet at distances of the order of ℓ or less, the collisions with the carrier gas do not hinder the reactant transport. Consequently, inside the region $a < r < R \propto \ell$ (R is referred to hereafter as the radius of the limiting sphere), the reactant molecules move in the free molecule regime. The value of R must be found from different consideration. Fuchs and Sutugin [21] proposed to determine this value from the numerical solution of the BGK equation; see, e.g., [22]. An improved version of the Fuchs interpolation formula [20] was obtained in Ref. [23] in the near-continuum regime by solving the Boltzmann equation using the momentum method.

B. Trapping efficiency

The latest modification of the Fuchs theory [16,18] includes the solution of the diffusion equation with a fixed flux J in the diffusion zone $r > R$, the solution of the collisionless Boltzmann equation in the free molecular zone $r < R$, and determining the radius of the limiting sphere from the condition of equality of the fluxes in both zones. The expression for $\alpha(a)$ was found in Ref. [18] for $n_+ = 0$ and $S_p = 1$:

$$\alpha(a) = \frac{2\pi a^2 v_T}{1 + \sqrt{1 + \left(\frac{a v_T}{2 D_G}\right)^2}}, \tag{4}$$

where D_G is the reactant diffusivity in the carrier gas. The extension of this formula to the case $n_+ \geqslant 0$ and $S_p \leqslant 1$ reads (for details, see [16])

$$\alpha(a) = \frac{S_p \pi a^2 v_T}{1 + \frac{S_p}{2}\left[\sqrt{1 + \left(\frac{a v_T}{2 D_G}\right)^2} - 1\right]}. \quad (5)$$

The radius R of the limiting sphere is found from the condition of the equality of the flux in the diffusion region and the flux in the free molecular region. This condition yields the formula for the radius of the limiting sphere [16,18]:

$$R = \sqrt{a^2 + \left(\frac{2 D_G}{v_T}\right)^2}. \quad (6)$$

It must be noted that R is independent of S_p and n_+. The spherical surface with radius R separates between the zones of the free-molecular and the continuous flow regimes. The value of $2D_G/v_T$ is of the order of ℓ, the reactant molecule mean free path. Hence, if $a \simeq \ell$ or less, then the radius R is of the order of $R \simeq \ell$.

The concentration profile of the reactant $n(r)$ in the gaseous phase inside the limiting sphere $a < r < R$ is continuous at $r = R$ together with its first derivative and is given by the following formula [18]:

$$\frac{n(r) - n_+}{n_\infty - n_+} = \left(1 - \frac{\alpha(a)}{4\pi D_G R}\right) \frac{b(r)}{b(R)}, \quad (7)$$

where

$$b(r) = 1 - \frac{S_p}{2}\left(1 - \sqrt{1 - \frac{a^2}{r^2}}\right). \quad (8)$$

Outside the limiting sphere at $r \geqslant R$,

$$\frac{n(r) - n_+}{n_\infty - n_+} = 1 - \frac{\alpha(a)}{4\pi D r}. \quad (9)$$

Note that the number density $n(a)$ is always larger than n_+. The formula for the concentration jump at the particle surface reads [16]

$$\Delta_a = n(a) - n_+ = (n_\infty - n_+)\left(1 - \frac{\alpha(a)}{4\pi D_G R}\right) \frac{b(a)}{b(R)}. \quad (10)$$

Inspection of Eq. (5) shows that when $a v_T / 2 D_G \gg 1$, $\alpha(a) = 4\pi a D_G$, and Eq. (5) recovers the Maxwell equation for the molecular flux in the continuum regime J_c:

$$J_c = 4\pi a D_G (n_\infty - n_+). \quad (11)$$

In Fig. 1, we showed the dependence of the ratio J/J_c versus the Knudsen number Kn for different values of the accommodation coefficient S_p (S_p was assumed to be 0.1, 0.2, 0.5, and 1.0 and $D_G \simeq 10^{-5}$ m^2/s).

As can be seen from this plot, the role of the kinetic effects can be significant for Kn $\gtrsim 0.1$.

Comparison of mass transfer rates as a function of Kn predicted by different theories [18,20,21,23] is shown in Fig. 2. As can be seen from Fig. 2, all approaches yield approximately the same results for small Kn numbers, Kn $\lesssim 0.1$, and for Kn $\gtrsim 10$.

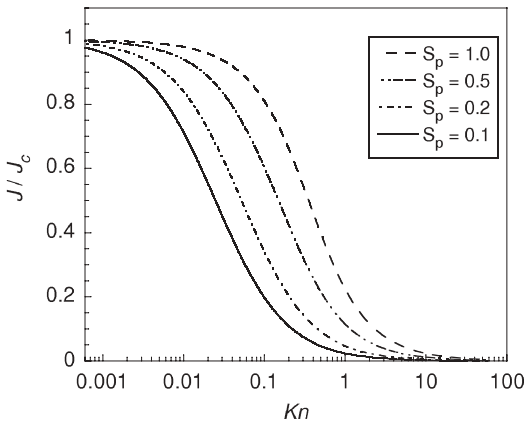

FIG. 1. Ratio of the molecular flux to the molecular flux in a continuum regime, J/J_c, as a function of Knudsen number Kn.

C. Inner diffusion-reaction equation

Consider now the effect of the first-order chemical reaction, e.g., chemical reaction dissociation, inside the droplet on the reactant flux toward the droplet. It is assumed that the concentration of the trace soluble gas is much smaller than the concentration of the carrier gas. Consequently, the approximation of infinite dilution of the soluble gas in a liquid phase can be applied. Neglecting recombination, the number density of reactant molecules inside the particle $n_L(r,t)$ is governed by the linear diffusion-reaction equation:

$$\frac{\partial n_L}{\partial t} = D_L \Delta n_L - \lambda n_L, \quad (12)$$

where $n_L = n_L(r,t)$ is the number density of reactant molecules inside the particle, D_L is the reactant diffusivity in the liquid phase, and λ is the dissociation rate. Equation (12) must be supplemented with the initial condition

$$n_L(r,0) = 0 \quad (13)$$

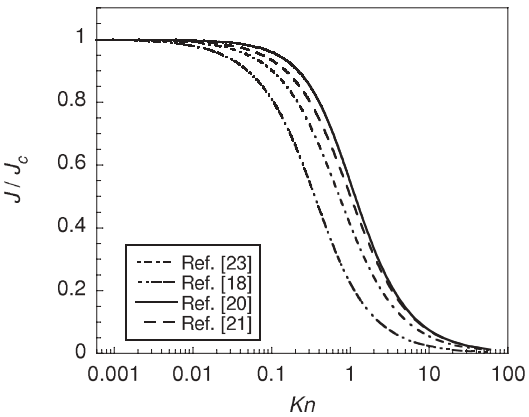

FIG. 2. Ratio of the molecular flux to the molecular flux in a continuum regime, J/J_c, as a function of Knudsen number Kn: ——, [20]; – – –, [21]; – · –, [23]; – ·· –, [18]. Accommodation coefficient $S_p = 1$.

(no reactant inside the droplet at $t = 0$) and the boundary conditions

$$\left.\frac{\partial n_L(r,t)}{\partial r}\right|_{r=0} = 0 \tag{14}$$

and

$$j(t) = -D_L \left.\frac{\partial n_L(r,t)}{\partial r}\right|_{r=a}, \tag{15}$$

where $j = j(t)$ is the flux density $j = J/(4\pi a^2)$ and J is the total flux.

Equation (12) together with the initial and boundary conditions (13)–(15) can be solved analytically (see Appendix). The result is the concentration profile $n_L(r,t)$ as a linear functional of $j(t)$. Substituting the determined concentration distribution $n_L(r,t)$ into the boundary condition, Eq. (15), yields the integral equation of Volterra type [24] for $j(t)$:

$$j(t) = \frac{\alpha(a)}{4\pi a^2}\left[n_\infty - \mathcal{H}\int_0^t S(t-t')j(t')dt'\right], \tag{16}$$

where

$$S(\xi) = 2\sum_{n>0} e^{-[D_L(\mu_n/a)^2+\lambda]\xi} + 3e^{-\lambda\xi} \tag{17}$$

and μ_n is the infinite set of the roots of the following transcendental equation:

$$\mu = \tan(\mu). \tag{18}$$

Equation (16) can be rewritten in dimensionless form for the dimensionless flux $j^*(\tau) = j(t)4\pi a^2/\alpha(a)n_\infty$, $\tau = D_L t/a^2$:

$$j^*(\tau) = 1 - g(a)\int_0^\tau S^*(\tau-\tau')j^*(\tau')d\tau', \tag{19}$$

where $g(a) = \frac{3\alpha(a)\mathcal{H}}{4\pi a D_L}$ and

$$S^*(\tau-\tau') = e^{-\mathrm{Da}(\tau-\tau')}\left[1 + \frac{2}{3}\sum_{n=1}^{\infty} e^{-\mu_n^2(\tau-\tau')}\right]. \tag{20}$$

In Eqs. (19) and (20), $\mathrm{Da} = \lambda a^2/D_L$ is Damkohler number, $\mathcal{H} = (H_A\mathcal{R}T)^{-1}$, H_A is Henry's law constant, $\mathcal{R}$ is a universal gas constant, and T is the temperature in the gaseous phase.

III. NUMERICAL METHOD

For the solution of the integral equation (19) we use the method based on the approximation of the integral in Eq. (19) using some quadrature formula:

$$\int_a^b F(x)dx = \sum_{j=1}^{n} A_j F(x_j)dx + R_n(F), \tag{21}$$

where $x_j \in [a,b]$, $j = 1,2,\ldots,n$, A_j are the coefficients associated with a family of quadrature rules, and $R_n(F)$ is a corresponding residuum. Taking successively $x = x_i$ $(i = 1,\ldots,n)$ and using the quadrature formula after discarding the terms $R_n(F_i)$ $(i = 1,\ldots,n)$, we obtain the following system of linear algebraic equations:

$$j_i^* - g(a)\sum_{j=1}^{n} A_j S_{ij}^* j_j^* = 1 \quad (i = 1,\ldots,n). \tag{22}$$

The solution of Eqs. (22) yields the approximative value of the unknown function j_i at the mesh point τ_i. The system of Eqs. (22) can be written in the following form:

$$-\sum_{j=1}^{i-1} A_j K_{ij} j_j^* + (1 - A_i K_{ii})j_i^* = 1, \tag{23}$$

where $K_{ij} = g(a)S_{ij}^*$. In a matrix form, the system of Eqs. (22) can be written as follows:

$$\begin{pmatrix} 1-A_1K_{11} & 0 & \cdots & 0 \\ -A_1K_{21} & 1-A_2K_{22} & \cdots & 0 \\ \vdots & & \ddots & \\ -A_1K_{n1} & -A_2K_{n2} & \cdots & 1-A_nK_{nn} \end{pmatrix}\begin{pmatrix} j_1^* \\ j_2^* \\ \vdots \\ j_n^* \end{pmatrix} = \begin{pmatrix} 1 \\ 1 \\ \vdots \\ 1 \end{pmatrix}. \tag{24}$$

Using the unequally spaced mesh with an increment $h_i = \tau_i - \tau_{i-1}$, $i = 2,\ldots,n$ and applying the trapezoidal integration rule Eqs. (22) yield the following recurrent equations:

$$j_1^* = 1, \quad j_2^* = \frac{1 + \frac{h_2}{2}K_{21}j_1^*}{1 - \frac{h_2}{2}K_{22}},$$
$$j_i^* = \frac{1 + \frac{h_2}{2}K_{i1}j_1^* + \sum_{j=2}^{i-1}\left(\frac{\tau_{j+1}-\tau_{j-1}}{2}\right)K_{ij}j_j^*}{1 - \frac{h_i}{2}K_{ii}} \quad (i = 3,\ldots,n). \tag{25}$$

Equations (25) are valid in the case in which $h_i \neq \frac{2}{K_{ii}}$.

In the numerical calculations, we spaced the mesh points adaptively using the following formula:

$$\tau_i = \tau_1 + (\tau_N - \tau_1)\left[1 - \cos\left(\frac{\pi}{2}\frac{i-1}{N-1}\right)\right] \quad (i = 1,2,\ldots,N). \tag{26}$$

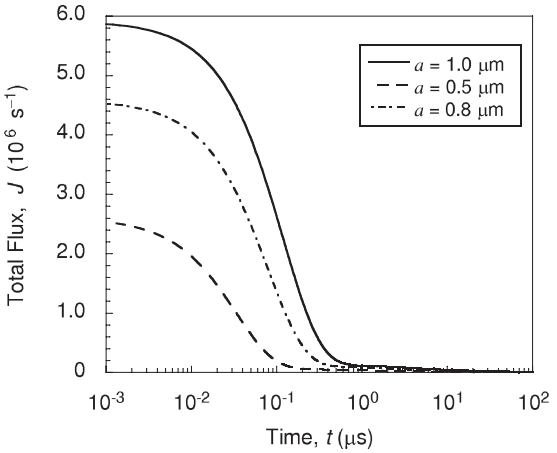

FIG. 3. Total molecular flux of sulfur dioxide as a function of time (droplet radii $a = 1.0$, 0.8, and 0.5 μm).

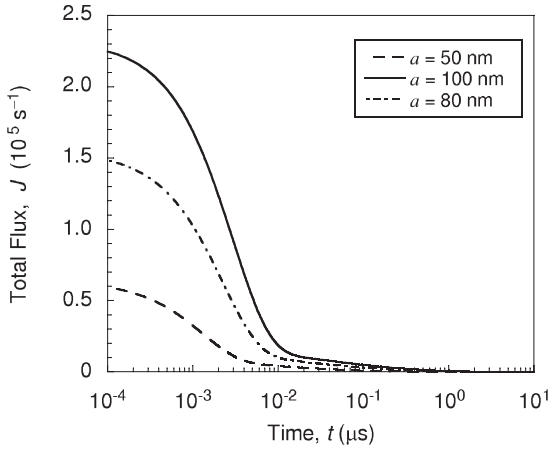

FIG. 4. Total molecular flux of sulfur dioxide as a function of time (droplet radii $a = 100.0$, 80.0, and 50.0 nm).

In Eq. (26), N is the chosen number of mesh points, and τ_1 and τ_N are the locations of the left and right boundaries of the time interval, respectively.

IV. RESULTS AND DISCUSSION

Using the suggested model, the calculations were performed for sulfur dioxide (SO_2), dinitrogen trioxide (N_2O_3), and chlorine (Cl_2) absorption by water aerosol particles. To validate our model, we compared the results obtained using the suggested model with the results obtained in our previous study for large droplets (Kn $\ll 1$) (see, e.g., [12]). The calculations were performed for the SO_2 absorption by a nonevaporating water droplet of 10 μm in radius. The concentration of sulfur dioxide in ambient air was assumed to be 0.01 ppm. The calculations showed that the time of the complete saturation of a droplet by sulfur dioxide estimated using the suggested model is $\approx$0.08 s, while the time of complete saturation of a droplet by sulfur dioxide estimated using our previous model is $\approx$0.1 s. These calculations demonstrate that the results obtained by both models are in fairly good agreement.

The results of calculation of the total mass flux of sulfur dioxide as a function of time are shown in Figs. 3 and 4.

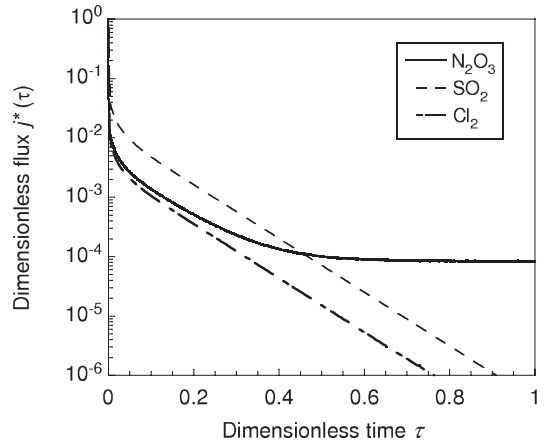

FIG. 5. Dimensionless molecular flux density $j^*(\tau)$ as a function of dimensionless time τ (radius of the droplet $a = 100$ nm).

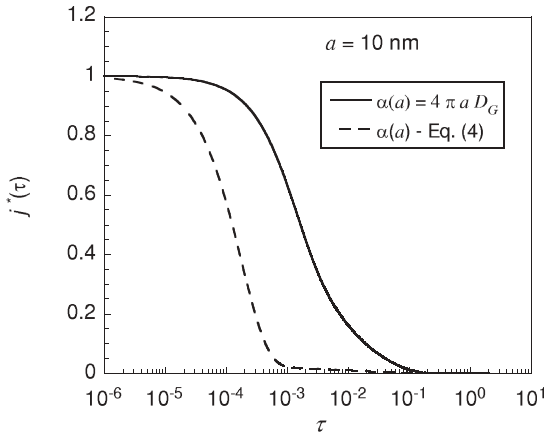

FIG. 6. Dimensionless molecular flux density $j^*(\tau)$ as a function of dimensionless time τ [solid line, $\alpha(a) = 4\pi a D_G$; dashed line, $\alpha(a)$ calculated using Eq. (4)].

The calculations were performed for various radii of a water aerosol particle (from 0.5 to 1.0 μm, $0.07 \lesssim$ Kn $\lesssim 0.14$, see Fig. 3, and from 50 to 100 nm, $0.7 \lesssim$ Kn $\lesssim 1.42$, see Fig. 4).

As can be seen from these plots for small and moderate sized droplets, the flux of absorbate decreases rapidly at the initial stage of gas absorption and approaches zero asymptotically at the final stage of the process. The vanishing flux of the absorbate implies the stage of saturation of a droplet by gas.

The results of calculation of the dimensionless flux $j^*(\tau) = j(t)4\pi a^2/\alpha(a)n_\infty$ as a function of dimensionless time $\tau = D_L t/a^2$ for different gases such as sulfur dioxide, chlorine, and dinitrogen trioxide are shown in Fig. 5. Larger values of mass flux at the later stages of gas absorption for N_2O_3 in comparison with SO_2 and Cl_2 absorption can be explained by large values of the constant of chemical reaction for N_2O_3 gas absorption in water ($\lambda_{N_2O_3} = 1.2 \times 10^4$ s^{-1}, $\lambda_{SO_2} = 10^{-3}$ s^{-1}, and $\lambda_{Cl_2} = 13.3$ s^{-1}).

Enhanced depletion of the dissolved gaseous N_2O_3 in a water droplet due to chemical reaction leads to a decrease of N_2O_3 concentration in the bulk of a water droplet and to an increase of the concentration gradient at the interface in a liquid phase. These two factors increase the mass transfer

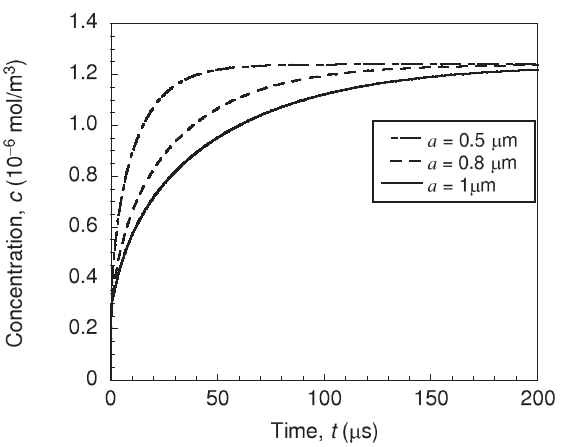

FIG. 7. Concentration of the dissolved SO_2 in the bulk of a droplet as a function of time (radii of a droplet 0.5, 0.8, and 1.0 μm).

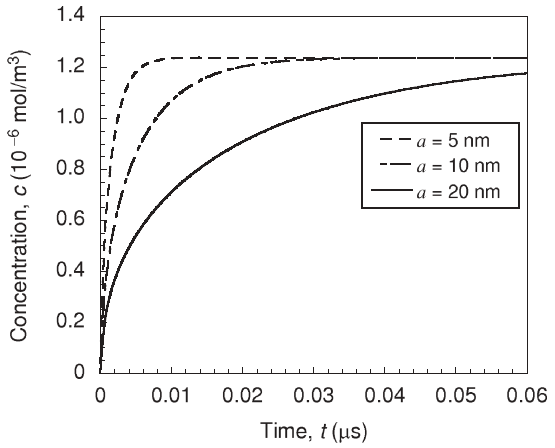

FIG. 8. Concentration of the dissolved SO_2 in the bulk of a droplet as a function of time (radii of a droplet 5.0, 10.0, and 20.0 nm).

coefficient in a droplet and increase the driving force of mass transfer in liquid.

As was mentioned above in the case of large droplets (Kn $\ll$ 1), the capture efficiency [see Eqs (4) and (5)] can be expressed by $\alpha(a) = 4\pi a D_G$. Consequently, the flux of soluble gas in a gaseous phase is expressed by an equation similar to Maxwell's equation [see Eq. (11)]. In Fig. 6, we showed the results of calculation of the dimensionless flux $j^*(\tau)$ of sulfur dioxide as a function of the dimensionless time τ. It was assumed that the concentration of sulfur dioxide in a gaseous phase is equal to 1 ppb, the temperature in a gaseous phase is 298 K, and the radius of a water nanoparticle is equal to 10 nm. The dashed line presents the results of calculation when the capture efficiency was calculated using Eq. (5). In our calculations, we assumed that the accommodation coefficient $S_p = 1$. The solid line present the results of calculation without using the kinetic approach, and thereby the capture efficiency was assumed to be equal to $\alpha(a) = 4\pi a D_G$. As can be seen from these plots, neglecting kinetic effects in the case of gas absorption by nanoaerosols can lead to an essential overestimation of mass flux.

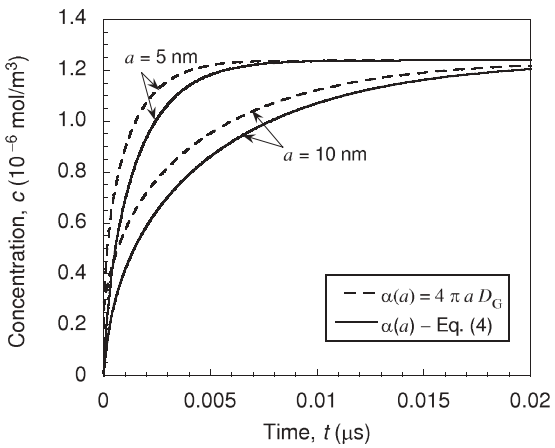

FIG. 9. Effect of Knudsen layer on temporal evolution of concentration of the dissolved SO_2 for droplets with the radii 5.0 and 10.0 nm.

Dependence of the average concentration of soluble sulfur dioxide in a droplet versus time is shown in Figs. 7 and 8. Calculations were performed for water droplets with the radii 0.5, 0.8, and 1 μm (Fig. 7) and for water droplets of radii 5, 10, and 20 nm (Fig. 8).

In these calculations, we employed the kinetic approach by using Eq. (5) for the capture efficiency $\alpha(a)$ with $S_p = 1$. In Fig. 9, the dependence of average concentration of SO_2 in a droplet versus time was calculated using the kinetic approach (solid lines) and neglecting kinetic effects (dashed lines). Calculations were performed for the droplets with the radii 10 and 5 nm. As can be seen from these plots, neglecting kinetic effects leads to a significant overestimation of the concentration of the dissolved gas in a droplet during the entire period of gas absorption. Clearly, when the duration of gas absorption $t \to \infty$, both approaches yield the same result for the magnitude of the dissolved gas concentration.

V. CONCLUSIONS

In this study, we developed a model for absorption of soluble trace gases by nanoaerosols taking into account dissociation reaction of the first order in a liquid phase. In the case in which the radius of the particle is comparable with the mean free path, transport of reactant molecules cannot be described by Fickian diffusion. However, application of the flux-matching theory allowed using the transient diffusion equation with the kinetic boundary conditions for the description of gas absorption by nanoaerosols. The transient diffusion equation was solved analytically and we derived a linear integral equation of Volterra type for the transient mass flux to a liquid droplet. The integral equation was solved numerically by the method based on the approximation of the integral using the quadrature formula with unequally spaced mesh.

The comparison of the suggested model with our earlier model developed for gas absorption by large droplets (Kn $\ll$ 1) (see [12]) showed that both models require the same amount of time for complete saturation of a large droplet by the soluble gas. Using the suggested model, we studied absorption of sulfur dioxide (SO_2), dinitrogen trioxide (N_2O_3), and chlorine (Cl_2) by water nanoaerosol. It was shown that enhanced depletion of the dissolved N_2O_3 gas in a water droplet due to a chemical reaction leads to a decrease of N_2O_3 concentration in the bulk of a water droplet and to an increase of the concentration gradient at the gas-liquid interface. Consequently, the flux of dinitrogen trioxide into a droplet is higher than the fluxes of sulfur dioxide and chlorine at later stages of gas absorption. It was demonstrated that neglecting kinetic effects leads to a significant overestimation of the soluble gas flux into a droplet during the entire period of gas absorption.

APPENDIX: DERIVATION OF THE INTEGRAL EQUATION OF VOLTERRA TYPE FOR THE MOLECULAR FLUX DENSITY

Here we give the details of the derivation of Eq. (16). Let us first remove j from the boundary condition (15). To this end,

let us introduce the unknown function $C(r,t)$:

$$n_L = C(r,t) - \frac{j(t)r}{D_L}. \tag{A1}$$

Substituting Eq. (A1) into Eq. (12), and taking into account that in spherical coordinates the Laplacian $\Delta r = 2/r$, we obtain the following equation for $C(r,t)$:

$$\frac{\partial C}{\partial t} = D_L \Delta C + \frac{r j_t}{D_L} - \frac{2j}{r} - \lambda C + \frac{\lambda j r}{D_L}, \tag{A2}$$

with the following boundary conditions:

$$\left.\frac{\partial C}{\partial r}\right|_{r=a} = 0 \tag{A3}$$

and

$$\left.\frac{\partial C}{\partial r}\right|_{r=0} = \left.\frac{j}{D_L}\right|_{r=0}. \tag{A4}$$

The substitution

$$C(r,t) = \frac{\chi(r,t)}{r} \tag{A5}$$

reduces Eq. (A2) to

$$\frac{\partial \chi}{\partial t} = D_L \frac{\partial^2 \chi}{\partial r^2} - \lambda \chi - 2j + \frac{1}{D_L}(r^2 j_t + \lambda j r^2). \tag{A6}$$

The boundary conditions to Eq. (A6) read

$$\left.\frac{\partial \chi}{\partial r}\right|_{r=a} - \left.\frac{\chi}{r}\right|_{r=a} = 0 \tag{A7}$$

and

$$\chi|_{r=0} = 0. \tag{A8}$$

Let us introduce the eigenfunctions

$$\frac{d^2\phi_n}{dr^2} = -\kappa^2 \phi_n, \tag{A9}$$

where the boundary conditions to Eq. (A9) are the same as for χ, i.e., they are given by Eqs. (A7) and (A8),

$$\left.\frac{\partial \phi_n}{\partial r}\right|_{r=a} - \left.\frac{\phi_n}{r}\right|_{r=a} = 0, \quad \phi_n|_{r=0} = 0. \tag{A10}$$

Then the solution of Eq. (A9) reads

$$\phi_n = u_n \sin\left(\mu_n \frac{r}{a}\right), \tag{A11}$$

where $\mu = \kappa a$ is the infinite set of the roots of the characteristic equation:

$$\mu = \tan(\mu). \tag{A12}$$

The roots μ_n of Eq. (A12) can be calculated numerically and are as follows: $\mu_1 = 4.4934$, $\mu_2 = 7.7253$, $\mu_3 = 10.9041$, $\mu_4 = 14.0662$, $\mu = 17.2208$, etc. The orthogonality condition for eigenfunctions reads

$$\int_0^a \phi_n \phi_m dr = \delta_{nm}, \tag{A13}$$

where δ_{nm} is the Kronecker delta. Equation (A13) allows us to determine the normalization constant u_n:

$$u_n^2 = \left(\int_0^a \sin^2\left(\mu_n \frac{r}{a}\right) dr\right)^{-1} = \frac{2}{a \sin^2 \mu_n}. \tag{A14}$$

The eigenvalue $\mu_n = 0$ [which is also the solution of Eq. (A12)] and the respective eigenfunction require special consideration. The solution of Eq. (A9) for $\mu_n = 0$ reads

$$\phi_0(r) = u_0 r, \tag{A15}$$

where the normalization constant u_0 is determined from (A13):

$$u_0 = \sqrt{\frac{3}{a^3}}. \tag{A16}$$

Let us now look for the solution to Eq. (A6) in the following form:

$$\chi(r,t) = 2\Psi_0(t)\phi_0 + \sum_{n>0} \Psi_n(t)\phi_n(r), \tag{A17}$$

where the coefficient 2 appears due to double degeneration of the eigenvalue $\mu_n = 0$. The equation for Ψ_n reads

$$\frac{d\Psi_n}{dt} = -\sigma_n \Psi_n + \frac{1}{D_L}(j_t + \lambda j) b_n - 2 j a_n, \tag{A18}$$

where

$$\sigma_n = \lambda + D_L \left(\frac{\mu_n}{a}\right)^2, \quad a_n = u_n \int_0^a \sin\left(\mu_n \frac{r}{a}\right) dr,$$
$$b_n = u_n \int_0^a r^2 \sin\left(\mu_n \frac{r}{a}\right) dr, \tag{A19}$$

and

$$\sigma_0 = \lambda, \quad a_0 = u_0 \int_0^a r\, dr = \frac{1}{2}\sqrt{3a},$$
$$b_0 = u_0 \int_0^a r^3 dr = \frac{1}{4}\sqrt{3a^5}. \tag{A20}$$

For $n > 0$, we obtain

$$\Psi_n(t) = \frac{b_n j(t)}{D_L} - \left[\left(\frac{\mu_n}{a}\right)^2 b_n + 2a_n\right] \int_0^t j(t') e^{-\sigma_n (t-t')} dt' \tag{A21}$$

and

$$\Psi_0(t) = \frac{b_0 j(t)}{D_L} - 2a_0 \int_0^t j(t') e^{-\lambda(t-t')} dt' \tag{A22}$$

for $n = 0$. The number density of molecules A inside the particle near the surface reads

$$n_-(a,t) = \frac{\chi(a,t)}{a} - \frac{j(t)a}{D_L}. \tag{A23}$$

Now let us determine χ from Eq. (A17). Noting that

$$\sum_{n\geqslant 0} b_n \phi_n(a) = \frac{a^2}{4} \tag{A24}$$

and

$$\left[\left(\frac{\mu_n}{a}\right)^2 b_n + 2a_n\right] \phi_n(a) = 2, \quad n > 0, \tag{A25}$$

$$\left[\left(\frac{\mu_n}{a}\right)^2 b_n + 2a_n\right] \phi_n(a) = 3, \quad n = 0, \tag{A26}$$

and using Eqs. (A17) and (A21)–(A23), we arrive at the following equation:

$$n_-(a) = -2\sum_{n>0}\int_0^t e^{-\sigma_n(t-t')}j(t')dt' - 3\int_0^t e^{-\lambda(t-t')}j(t')dt'. \tag{A27}$$

According to Henry's law, $n_+ = \mathcal{H}n_-$. Using the equation for the flux density,

$$j(t) = \frac{1}{4\pi a^2}\alpha(a)(n_\infty - n_+), \tag{A28}$$

we arrive at the following integral equation of Volterra type for $j(t)$:

$$j(t) = \frac{\alpha(a)}{4\pi a^2}\left[n_\infty - \mathcal{H}\int_0^t S(t-t')j(t')dt'\right], \tag{A29}$$

where the kernel $S(t-t')$ is given by the following formula:

$$S(\xi) = 2\sum_{n>0} e^{-[D_L(\mu_n/a)^2+\lambda]\xi} + 3e^{-\lambda\xi}. \tag{A30}$$

[1] R. Zhang, A. Khalizov, L. Wang, M. Hu, and W. Xu, Chem. Rev. **112**, 1957 (2012).

[2] M. Kulmala, H. Vehkamäki, T. Petäjä, M. Dal Maso, A. Lauri, V.-M. Kerminen, W. Birmili, and P. H. McMurry, Aerosol Sci. **35**, 143 (2004).

[3] M. Krämer, N. Beltz, D. Schell, L. Schütz, C. Sprengard-Eichel, and S. Wurzler, J. Geophys. Res. **105**, 11739 (2000).

[4] H. R. Pruppacher and J. D. Klett, *Microphysics of Clouds and Precipitation*, 2nd ed. (Kluwer, Dordrecht, 1997).

[5] A. I. Flossmann, Pure Appl. Chem. **70**, 1345 (1998).

[6] J. H. Seinfeld and S. N. Pandis, *Atmospheric Chemistry and Physics. From Air Pollution to Climate Change*, 2nd ed. (Wiley, New York, 2006).

[7] K. L. Hayden, A. M. Macdonald, W. Gong, D. Toom-Sauntry, K. G. Anlauf, A. Leithead, S. M. Li, W. R. Leaitch, and K. Noone, J. Geophys. Res. **113**, D18201 (2008).

[8] I. Taniguchi and K. Asano, J. Chem. Eng. Jpn. **25**, 614 (1992).

[9] R. Clift, J. R. Grace, and M. E. Weber, *Bubbles, Drops and Particles* (Academic, New York, 1978).

[10] S. E. Schwartz and J. E. Freiberg, Atmos. Environ. **15**, 1129 (1981).

[11] T. Elperin, A. Fominykh, and B. Krasovitov, J. Atmos. Sci. **64**, 983 (2007).

[12] T. Elperin, A. Fominykh, and B. Krasovitov, Atmos. Environ. **42**, 3076 (2008).

[13] C. F. Clement, in *Environmental Chemistry of Aerosols*, edited by I. Colbeck (Wiley Interscience, New York, 2007), pp. 49–89.

[14] J. Geng, C. Nie, and H. W. Marlow, Int. J. Heat Mass Transf. **55**, 2429 (2012).

[15] U. Pöschl, Y. Rudich, and M. Ammann, Atmos. Chem. Phys. **7**, 5989 (2007).

[16] A. A. Lushnikov, *Nanoaerosols in the Atmosphere*, in *The Atmosphere and Ionosphere. Elementary Processes, Discharges and Plasmoids. Physics of Earth and Space Environment*, edited by V. Bychkov, G. Golubkov, and A. Nikitin (Springer, Dordrecht, 2013), Chap. 3.

[17] T. Vesala, A. U. Hannemann, B. P. Luo, M. Kulmala, and Th. Peter, Aerosol Sci. **32**, 843 (2001).

[18] A. A. Lushnikov and M. Kulmala, Phys. Rev. E **70**, 046413 (2004).

[19] P. E. Wagner, *Aerosol Growth by Condensation*, in *Aerosol Microphysics, II: Chemical Physics of Microparticles*, edited by W. H. Marlow (Springer, Berlin, 1982), Chap. 5, pp. 129–178.

[20] N. A. Fuchs, in *The Mechanics of Aerosols*, edited by C. N. Davies (MacMillan, New York, 1964).

[21] N. A. Fuchs and A. G. Sutugin, in *Topics in Current Aerosol Research*, edited by G. M. Hidy and J. R. Brock, Vol. 2 (Pergamon, Oxford, 1971), pp. 1–60.

[22] D. C. Sahni, J. Nucl. Energy. Parts A/B **20**, 915 (1966).

[23] S. K. Loyalka, J. Colloid Interface Sci. **87**, 216 (1982).

[24] A. Apelblat, *Volterra Functions* (Nova Science, New York, 2008).